

An Efficient, High-Rate Scheme for Private Information Retrieval over the Gaussian MAC

Or Elimelech and Asaf Cohen

Department of Electrical & Computer Engineering
Ben-Gurion University of the Negev Beersheba, Israel

Abstract—This paper revisited the problem of Private Information Retrieval (PIR), where there are N replicated non-communicating databases containing the same M messages and a user who wishes to retrieve one of the messages without revealing the wanted message's index to the databases. However, we assume a block-fading additive white Gaussian noise multiple access channel (AWGN MAC) linking the user and the databases. Previous work [1] presented a joint channel-PIR scheme, utilizing the Compute and Forward protocol, showing the potential of a joint channel-PIR scheme over a separated one. This paper proposes an improved joint scheme tailored for the PIR problem with N databases over a block-fading AWGN. Unlike the C&F protocol, our scheme offers reduced computational complexity while improving the scaling laws governing the achievable rate. Specifically, the achievable rate scales with the number of databases N and the power P similarly to the channel capacity without the privacy constraint and outperforms the C&F-based approach. Furthermore, the analysis demonstrates that the improved rate exhibits only a finite gap from the unconstrained channel capacity – one bit per second per Hz as N increases.

Index Terms—Private Information Retrieval, Multiple Access Channel, Lattice Codes, Gaussian channel.

I. INTRODUCTION

Private Information Retrieval (PIR) is a protocol that enables a user to retrieve a data item from a database while preserving the privacy of the item identity that has been retrieved.

Extensive research on Private Information Retrieval (PIR) has been conducted within the Computer Science community, with notable contributions from [2]–[4]. The primary focus of these studies has been on computational solutions, leading to the development of computational PIR (cPIR). Recently, the information theory community has also turned its attention to PIR, offering a slightly different interpretation aimed at understanding the problem's fundamental limits. The information-theoretic approach to PIR emphasizes privacy to such an extent that the identity of the desired message remains concealed even against unlimited computational power. Moreover, an information-theoretic perspective usually assumes large enough messages, neglecting the price of communicating the queries themselves.

In recent years, the relevance of the PIR problem has continued to grow, driven by the increasing need for privacy-preserving information retrieval in various domains. For example, in the field of machine learning, PIR has gained attention as a means to securely access distributed datasets while maintaining data privacy [5]–[7].

In the fundamental setup, there are N identical databases (or servers), each containing the same M messages. These servers do not communicate with each other. A user who wishes to retrieve a specific message without revealing its identity to the servers formulates a series of queries. The servers respond truthfully to these queries. The goal is to reduce the overhead necessary for maintaining privacy.

The pioneering work by the authors in [8] explored whether employing multiple databases could lead to a more efficient PIR solution. They demonstrated that in a single-server scenario, perfect information-theoretic privacy can only be attained by downloading the entire database. This means that for M messages, the PIR rate is $1/M$. They further established that when using only two servers ($N = 2$), the rate can be improved to $1/2$, irrespective of the number of messages M .

Numerous PIR schemes have drawn inspiration from the two-database scheme provided by [8]. Subsequently, [9] unveiled a renowned result for the PIR problem. They established that with the classic setting, the PIR capacity is given by $C_{PIR} = (1 - 1/N)(1 - (1/N)^M)$.

Building upon the foundation of PIR, various extensions have been developed to tackle its inherent complexities [10]–[19].

In [1], the authors addressed the problem of PIR over a Gaussian Multiple Access Channel (MAC), where the user communicates with the server through a block-fading Gaussian MAC. The authors proposed joint privacy and channel coding retrieval schemes that leveraged the linearity of the channel while using the Compute and Forward (C&F) coding scheme [20] and modulo-lattice additive noise (MLAN) channel technique [21]. Their approach demonstrated superior performance compared to the separation-based scheme, both with and without fading. However, it is important to note that their proposed solution is highly computationally complex. It requires a search over a discrete space in addition to a partitioning problem, and the achievable rate does not scale optimally with the power parameter P . This paper proposes an improved joint PIR scheme. Our suggested scheme overcomes the cons of the scheme presented in [1] in terms of computation complexity and scaling laws. By leveraging the additive nature of the channel and harnessing the linear properties and structure of lattice codes, our method achieves efficient and secure PIR at the physical layer.

II. SYSTEM MODEL AND PROBLEM STATEMENT

A. Notational Conventions

Throughout the paper, we will use boldface lowercase to refer to vectors, e.g., $\mathbf{h} \in \mathbb{R}^L$, and boldface uppercase to refer to matrices, e.g., $\mathbf{H} \in \mathbb{R}^{M \times L}$. For a vector \mathbf{h} , we write $\|\mathbf{h}\|$ for its Euclidean norm, i.e., $\|\mathbf{h}\| \triangleq \sqrt{\sum_i h_i^2}$. We denote by \mathbf{e}_i the unit vector with 1 at the i th entry and zero elsewhere. We assume that the log operation is with respect to base 2.

B. System Model

Consider the PIR problem in a basic setting with N non-communicating databases. Each database stores the same set of messages $W_1^M = \{W_1, W_2, \dots, W_M\}$, where W_m is an L -length vector picked uniformly from prime-size finite field \mathbb{F}_p^L , where p is a prime number. These messages are independent and identically distributed, i.e.,

$$\begin{aligned} H(W_l) &= L \log p \text{ for } l = 1, \dots, M, \\ H(W_1^M) &= ML \log p. \end{aligned} \quad (1)$$

In PIR, the user wishes to retrieve the message W_θ for some $\theta \sim U[1, \dots, M]$ while keeping θ a secret from each database. We denote the uniformly distributed message index as θ , yet use the index i to represent its specific realization. To achieve private retrieval, the user generates a set of N queries $Q_1(i), Q_2(i), \dots, Q_N(i)$, one for each database, where each query is statistically independent of the messages, i.e.,

$$I(W_1^M; Q_1(\theta), \dots, Q_N(\theta)) = 0. \quad (2)$$

The k th database responds to its query $Q_k(i)$ with a message (or codeword) $\mathbf{x}_k(i)$ of fixed size n . We follow the usual Gaussian MAC setup in the literature [22], where a codeword is transmitted during n channel uses. The response $\mathbf{x}_k(i)$ is a deterministic function of the messages and the query. Therefore, for each $k \in \{1, \dots, N\}$, we have:

$$H(\mathbf{x}_k(\theta) | W_1^M, Q_k(\theta)) = 0. \quad (3)$$

To ensure privacy, the query should not reveal the desired index i to the database. Thus, we impose the privacy constraint that for each database j , the random variable θ is independent of the query, the answer, and the messages:

$$I(\theta; Q_j(\theta), \mathbf{x}_j(\theta), W_1^M) = 0 \text{ for all } j \in \{1, \dots, N\}. \quad (4)$$

The databases are linked to the user via a block-memoryless fading AWGN channel. In this setup, the channel remains constant throughout the transmission of codewords of size n , and each block is independent of the others.

In this model, over a transmission of n symbols, the user observes a noisy linear combination of the transmitted signals,

$$\mathbf{y} = \sum_{k=1}^N h_k \mathbf{x}_k + \mathbf{z}$$

Here, $h_k \sim \mathcal{N}(0, 1)$ represents the real channel coefficients, and \mathbf{z} is an i.i.d. Gaussian noise $\mathbf{z} \sim \mathcal{N}(0, \mathbf{I}^{n \times n})$. We assume there is channel state information at the transmitter

(CSIT), i.e., $\{h_k\}_{k=1}^N$ are known at the transmitter. We also assume an average power constraint on the codewords, i.e., $\mathbb{E}[\|\mathbf{x}_k\|^2] \leq nP$.

Upon receiving the mixed response $\mathbf{y}(i)$ from all the databases, the user decodes the required message W_i . Let \widehat{W}_i denote the decoded message at the user and define the error probability for decoding a message as follows,

$$P_e(L) \triangleq P_r(\widehat{W}_i \neq W_i). \quad (5)$$

We require that $P_e(L) \rightarrow 0$ as L tends to infinity.

We assume that explicit cooperation among databases is not feasible. However, implicit cooperation is achievable by leveraging the user's queries. Additionally, we assume a per-database power constraint, where all transmitting databases operate with a fixed power P . This per-database power constraint aligns our model with the Multiple Input Single Output (MISO) channel with per-antenna power constraint, enabling each transmit antenna to have a separate power budget. The MISO sum capacity with per-antenna power constraint and fixed channel coefficients, which are globally known, is given by [23],

$$C_{SR}^{MISO} = \frac{1}{2} \log \left(1 + P \left(\sum_{k=1}^N |h_k| \right)^2 \right). \quad (6)$$

C. Performance Metric

The PIR rate is typically defined as the ratio between the number of desired bits and the total number of received bits. In the information-theoretic formulation, where the size of the messages is assumed to be arbitrarily large, the upload cost is negligible. Hence, the PIR rate can be expressed as:

$$R_{PIR} \triangleq \frac{L \log p}{D}, \quad (7)$$

Where D is the total number of bits that have been downloaded. However, counting the total number of downloaded bits is, by definition, suitable for cases where there is a separation between the PIR code and the channel code, or, in other words, the channels are clean and orthogonal. Thus, we define the PIR capacity over an AWGN MAC as follows.

Definition 1: Denote:

$$R_{PIR}^{MAC}(n) \triangleq \frac{H(W_i)}{n} = \frac{L \log p}{n},$$

where n represents the number of channel uses. The PIR capacity over AWGN MAC, denoted by C_{PIR}^{MAC} , is the supremum of $R_{PIR}^{MAC}(n)$, under which reliable communication is achievable, ensuring the privacy of the user's will. That is, satisfying (2,3,4) and (5).

Clearly, neglecting the privacy constraint reduces the problem to the MISO channel with per-antenna power constraint. Hence, it becomes natural to use Gaussian MISO channel capacity as an upper bound to the problem $C_{SR}^{MISO} \geq C_{PIR}^{MAC}$. In fact, we will see that comparing the PIR rate to the channel capacity without the privacy constraint is quite an interesting comparison, as C_{PIR}^{MAC} will approach it in several cases. It has been shown already by [1], [19] that separation between

the channel coding and the PIR coding is not always optimal when dealing with a MAC. Indeed, [1] showed that better overall performance can be achieved when the PIR and the channel coding are jointly designed.

In this paper, we propose a joint PIR scheme. The achievable rate is compared to the result in [1] and to the full channel capacity without any privacy constraint. The scheme improves the rate and significantly reduces the computational complexity. Notably, our approach eliminates the need to optimize over a discrete space, a requirement of the scheme presented in [1] which greatly increases complexity yet improves the scaling laws of the rate, and, furthermore, is shown to be only 1 bit away from the full, unconstrained capacity.

III. MAIN RESULTS

Theorem 1 states the main result of this work.

Theorem 1: *Consider the PIR problem with N databases over a block-fading AWGN. Then, for any non-empty subsets of databases $\mathcal{S}_1, \mathcal{S}_2$ satisfying $\mathcal{S}_1 \cap \mathcal{S}_2 = \emptyset$, $\mathcal{S}_1 \cup \mathcal{S}_2 \subseteq \{1, \dots, N\}$, the following PIR rate is achievable,*

$$R_{PIR}^{eq} = \frac{1}{2} \log^+ \left(\frac{1}{2} + \tilde{h}_1^2 P \right) \quad (8)$$

where, $\tilde{h}_i \triangleq \sum_{k \in \mathcal{S}_i} |h_k|$, $\tilde{h}_1 \leq \tilde{h}_2$.

In order to analyze the achievable PIR rate in Theorem 1, one should note that the user may choose \mathcal{S}_1 and \mathcal{S}_2 to maximize it. Namely, we have the following optimization problem,

$$\max_{\substack{\mathcal{S}_1, \mathcal{S}_2 \\ \tilde{h}_1 \leq \tilde{h}_2}} \left\{ \frac{1}{2} \log^+ \left(\frac{1}{2} + \left(\sum_{k \in \mathcal{S}_1} h_k \right)^2 P \right) \right\}.$$

To maximize the rate, the user has to choose \mathcal{S}_1 which maximize \tilde{h}_1 such that $\tilde{h}_1 \leq \tilde{h}_2$, which means partition \mathcal{S}_1 and \mathcal{S}_2 to bring \tilde{h}_1 as close as possible to \tilde{h}_2 . Finding the optimal solution is related to the subset sum problem, which is known to be NP-hard. To put Theorem 1 in context, we consider the gap from the MISO sum capacity, which does not assume any privacy constraint. The following lemma, whose proof is given in Appendix A, shows that the rate loss due to the privacy constraint is at most one bit per channel use for N large enough.

Lemma 1: *The PIR rate with N databases over a block-fading AWGN MAC given in Theorem 1 has a gap of at most $1 + O\left(\frac{1}{N}\right)$ bits from the channel capacity. That is,*

$$C_{SR}^{MISO} - \max_{\substack{\mathcal{S}_1, \mathcal{S}_2 \\ \tilde{h}_1 \leq \tilde{h}_2}} \{R_{PIR}^{eq}\} \leq 1 + O\left(\frac{1}{N}\right). \quad (9)$$

Thus, Lemma 1 asserts that the price paid for enforcing the privacy constraint is limited by 1 bit when the number of databases is large enough. This should be compared to the C&F based scheme suggested in [1], which achieves a similar result only for the case without fading. The price we pay in rate for the block fading case using the C&F based is caused mainly by mismatch alignment between the partitioned fading

coefficients \tilde{h}_1, \tilde{h}_2 and the wanted integer linear coefficients we try to decode. More details about it will be given in Section V.

IV. A PIR SCHEME FOR THE BLOCK-FADING AWGN-MAC

This section presents a new PIR scheme for the block-fading AWGN MAC.

A. Coding Scheme

Our scheme utilizes nested lattice codebooks, which are linear codes¹. Specifically, we construct a nested lattice codebook, as described in [20, Section 4.B], using two n -dimensional lattices denoted as Λ_c and Λ_f . These lattices Voronoi regions denoted as \mathcal{V}_c and \mathcal{V}_f , respectively, such that Λ_c is a subset of Λ_f , i.e., $\Lambda_c \subset \Lambda_f$. The nested lattice code is then given by $\mathcal{C} = \{\Lambda_f \cap \mathcal{V}_c\}$.

The code is known to the user and all the databases. Additionally, there exists a one-to-one mapping function, $\phi(\cdot)$, between a vector of l information bits and a lattice point $\lambda \in \mathcal{C}$ [20, Lemma 5], namely:

$$\mathbf{s} = (s_1, \dots, s_l) \in \{0, 1\}^l \mapsto \lambda = (\lambda_1, \dots, \lambda_n) \in \mathcal{C}.$$

Roughly speaking, in our proposed scheme, each database encodes its answer using a nested lattice code with a rate R that will be determined. This encoding ensures that the answers can be added constructively to retrieve the requested message while canceling all other messages.

The queries and the assignment to whom they are being sent differ and depend on the channel vector \mathbf{h} , determined by nature. Thus, Theorem 1 initially presents the result for a fixed \mathbf{h} and fixed subsets of users.

Proof of Theorem 1: Assume the user wants to retrieve message W_i privately. To do that, the user generates a random vector \mathbf{b} of length M such that each entry is either 1 or 0, independently and with equal probability. Then, the user divides the databases into two non-intersecting subsets, denoted as \mathcal{S}_1 and \mathcal{S}_2 , for which he sends the query $Q_1(i)$ to each member in \mathcal{S}_1 and $Q_2(i)$ to each member in \mathcal{S}_2 . The queries are given as follows

$$\begin{aligned} Q_1(i) &= \mathbf{b}, \quad Q_2(i) = -\mathbf{b} - \mathbf{e}_i, \text{ if } b_i = 0 \\ Q_1(i) &= \mathbf{b}, \quad Q_2(i) = -\mathbf{b} + \mathbf{e}_i, \text{ if } b_i = 1 \end{aligned} \quad (10)$$

From the databases' perspective, each sees a uniform random vector with elements 1 or 0 or either with elements -1 or 0 with equal probability. Thus, the privacy requirement in (4) is fulfilled. We assume the messages are long. Hence, the message is broken up into smaller, manageable chunks of information (packetization) $\mathbf{s}_{j,m} \in \{0, 1\}^l$ where $\mathbf{s}_{j,m}$ is the j th packet of W_m . These packets are then transmitted over the channel and reassembled by the receiver to form the original message. Hence, we focus on the transmission of the j th packet. The rest are transmitted the same way.

¹More details about lattice codes and the rationale behind their selection can be found in [1].

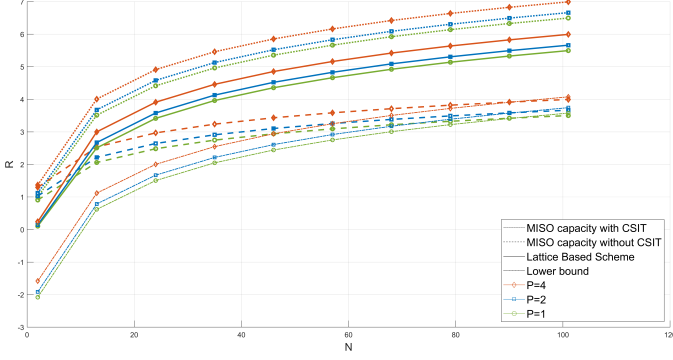


Fig. 1: The average PIR rate (solid lines) as a function of N .

The databases form their answers according to the received queries (10), as follows:

$$\begin{aligned} \mathbf{A}_k &= \left[\sum_{m=1}^M Q_{k,m}(i) \phi(\mathbf{s}_{j,m}) \right] \bmod \Lambda_c \\ \mathbf{A}_{k+1} &= \left[\sum_{m=1}^M Q_{k+1,m}(i) \phi(\mathbf{s}_{j,m}) \right] \bmod \Lambda_c \end{aligned} \quad (11)$$

where $\mathbf{s}_{j,m}$ represent the j th packets of W_m , $k \in \{1, 3, 5, \dots, 2 \lfloor \frac{N}{2} \rfloor - 1\}$; $Q_{k,m}(i)$ is the m th entry of the vector $Q_k(i)$; Note that $[\mathbf{A}_k + \mathbf{A}_{k+1}] \bmod \Lambda_c$ is equal to either $[\phi(\mathbf{s}_{j,i})] \bmod \Lambda_c = [\mathbf{v}] \bmod \Lambda_c$, or $[-\phi(\mathbf{s}_{j,i})] \bmod \Lambda_c = [-\mathbf{v}] \bmod \Lambda_c$ where \mathbf{v} is the lattice codeword for the private packet $\mathbf{s}_{j,i}$. This depends on the value of b_i , which is known to the user.

Assume, without loss of generality, $\tilde{h}_1 \leq \tilde{h}_2$, and let \mathbf{d}_1 and \mathbf{d}_2 be two mutually independent dithers which are uniformly distributed over the Voronoi region \mathcal{V}_c . The dithers are known to both the user and the servers. Then, each server transmits either \mathbf{x}_1 or \mathbf{x}_2 accordingly to the subset \mathcal{S}_l which it belongs, namely:

$$\begin{aligned} \mathbf{x}_1 &= [\mathbf{A}_1 - \mathbf{d}_1] \bmod \Lambda_c \\ \mathbf{x}_2 &= \frac{\tilde{h}_1}{\tilde{h}_2} \mathbf{x}'_2 = \frac{\tilde{h}_1}{\tilde{h}_2} [\mathbf{A}_2 - \mathbf{d}_2] \bmod \Lambda_c \end{aligned} \quad (12)$$

Using two dithers allows the distribution of \mathbf{x}_j and \mathbf{x}_{j+1} to be uniform on the Voronoi region and also to make them independent [21] [20]. The user may add additional information to the query, informing the server which group he belongs to and which dither to use in the encoding. This information does not affect the privacy constraint as shown in [1].

The received signal by the user is then given by:

$$\mathbf{y} = \sum_{k \in \mathcal{S}_1} h_k \mathbf{x}_1 + \sum_{k \in \mathcal{S}_2} h_k \mathbf{x}_2 + \mathbf{z} = \tilde{h}_1 (x_1 + x'_2) + \mathbf{z}$$

To decode \mathbf{v} , the user computes the following,

$$\hat{\mathbf{v}} = \left[\alpha \frac{1}{\tilde{h}_1} \mathbf{y} + \mathbf{d}_1 + \mathbf{d}_2 \right] \bmod \Lambda_c$$

where $0 \leq \alpha \leq 1$ needs to be optimized later.

To compute the expression, we transform the channel to the Modulo-Lattice Additive Noise (MLAN) channel [21] as follows,

$$\begin{aligned} \hat{\mathbf{v}} &= \left[\alpha \frac{1}{\tilde{h}_1} \mathbf{y} + \mathbf{d}_1 + \mathbf{d}_2 \right] \bmod \Lambda_c \\ &= \left[\alpha \frac{1}{\tilde{h}_1} (\tilde{h}_1 \mathbf{x}_1 + \tilde{h}_2 \mathbf{x}_2 + \mathbf{z}) + \mathbf{d}_1 + \mathbf{d}_2 \right] \bmod \Lambda_c \\ &= \left[\alpha \left(\mathbf{x}_1 + \frac{\tilde{h}_2}{\tilde{h}_1} \mathbf{x}_2 + \frac{1}{\tilde{h}_1} \mathbf{z} \right) + \mathbf{d}_1 + \mathbf{d}_2 \right] \bmod \Lambda_c \\ &= \left[\alpha \left(\mathbf{x}_1 + \mathbf{x}'_2 + \frac{1}{\tilde{h}_1} \mathbf{z} \right) + \mathbf{d}_1 + \mathbf{d}_2 \right] \bmod \Lambda_c \\ &\stackrel{(a)}{=} \left[\mathbf{x}_1 + \mathbf{x}'_2 + (\alpha - 1)(\mathbf{x}_1 + \mathbf{x}'_2) \right. \\ &\quad \left. + \alpha \frac{1}{\tilde{h}_1} \mathbf{z} + \mathbf{d}_1 + \mathbf{d}_2 \right] \bmod \Lambda_c \\ &= \left[[\mathbf{A}_1 - \mathbf{d}_1] \bmod \Lambda_c + [\mathbf{A}_2 - \mathbf{d}_2] \bmod \Lambda_c \right. \\ &\quad \left. - (1 - \alpha)(\mathbf{x}_1 + \mathbf{x}'_2) + \alpha \frac{1}{\tilde{h}_1} \mathbf{z} + \mathbf{d}_1 + \mathbf{d}_2 \right] \bmod \Lambda_c \\ &\stackrel{(b)}{=} \left[\mathbf{v} - (1 - \alpha)(\mathbf{x}_1 + \mathbf{x}'_2) + \alpha \frac{1}{\tilde{h}_1} \mathbf{z} \right] \bmod \Lambda_c \end{aligned}$$

where (a) is the MLAN equivalent channel. (b) follows from the distributive property of the $\bmod \Lambda_c$ operation and due to the structure of the answers (11) where we assume that $b_i = 1$. In case $b_i = 0$, we would result with negative sign to \mathbf{v} . Thus, since b_i is known to the user, he can correct $\hat{\mathbf{v}}$ by multiplying with -1 . Finally, we define the equivalent noise term $\mathbf{z}_{eq} \triangleq -(1 - \alpha)(\mathbf{d}_1 + \mathbf{d}_2) + \alpha \frac{1}{\tilde{h}_1} \mathbf{z}$. The second moment of \mathbf{z}_{eq} is approaching (for n large enough [20]) to $\sigma_{eq}^2 = \frac{1}{n} E[\|\mathbf{z}_{eq}\|^2] = 2P(1 - \alpha)^2 + \frac{1}{h_1^2} \alpha^2$; where we can

optimize it on α . Specifically, $\alpha_{opt} = \frac{2P}{2P + \frac{1}{h_1^2}}$; $\sigma_{opt}^2 = \frac{2P \frac{1}{h_1^2}}{2P + \frac{1}{h_1^2}}$. Therefore, the decoding error probability can be made arbitrarily small as the block length n tends to infinity, leading to an achievable rate of $R = \frac{1}{2} \log^+ \left(\frac{1}{2} + \tilde{h}_1^2 P \right)$. ■

As depicted in Figure 1, the PIR rate scales with N the same as the unconstrained channel capacity (For further details, see Appendix C). Moreover, the PIR rate exceeds the MISO capacity without CSIT and approaches the capacity with CSIT up to a constant gap. These results demonstrate that the PIR scheme can achieve rates close to the channel's capacity as P and N grow, affirming its efficiency and potential for practical applications.

B. Lower Bound on the Expected Achievable Rate

In order to maximize the Private Information Retrieval (PIR) rate as given by (8), it is crucial for the user to carefully

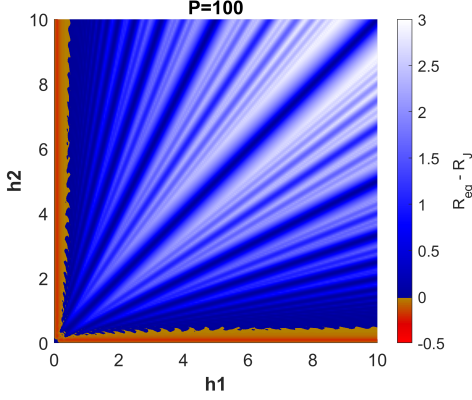


Fig. 2: The graphs shows the difference between R_{PIR}^{eq} to $R_{PIR}^{C\&F}$ for different \tilde{h}_1 and \tilde{h}_2 . black colors are for positive values, and red is for negative values.

choose \mathcal{S}_1 and \mathcal{S}_2 . This selection process leads us to a global optimization problem, which can be expressed as:

$$\max_{\substack{\mathcal{S}_1, \mathcal{S}_2 \\ \tilde{h}_1 \leq \tilde{h}_2}} \left\{ \frac{1}{2} \log^+ \left(\frac{1}{2} + \left(\sum_{k \in \mathcal{S}_1} h_k \right)^2 P \right) \right\} \quad (13)$$

An asymptotic lower bound on the expected PIR rate given by (13) is provided in the following theorem (the proof of which can be found in Appendix B):

Theorem 2: *The expected PIR rate in (13) is asymptotically lower-bounded by,*

$$\begin{aligned} \mathbb{E}[R_{PIR}^{eq, max}] &= \mathbb{E} \left[\max_{\substack{\mathcal{S}_1, \mathcal{S}_2 \\ \tilde{h}_1 \leq \tilde{h}_2}} \left\{ \frac{1}{2} \log^+ \left(\frac{1}{2} + \left(\sum_{k \in \mathcal{S}_1} h_k \right)^2 P \right) \right\} \right] \\ &\geq \frac{1}{2} \log \left(\frac{2 + N^2 P c}{4} \right) - o(1) \end{aligned} \quad (14)$$

where $c = \left(\sqrt{\frac{2}{\pi}} - \frac{1}{2} \right)^2$, $o(1) \rightarrow 0$ as $N \rightarrow \infty$.

The lower bound on the expected PIR rate given by Theorem 2 indicates that the PIR rate is an increasing function of the number of servers and the power gain. In fact, it scales the same as the MISO sum capacity with CSIT (6).

V. COMPARISON BETWEEN THE SCHEMES

We highlight the key technical distinction of our scheme from the scheme presented in [1]. In their scheme, the objective is to decode an integer linear combination of the transmitted server responses, aiming for the closest approximation to the actual linear combination received by the user, specifically, $\tilde{h}_1 \mathbf{x}_1 + \tilde{h}_2 \mathbf{x}_2 + \mathbf{z}$. Their decode stage leverages results from [20], [21]. In contrast, our proposed scheme takes a different approach. We design the server responses to ensure equal gains. In that way, we have to decode the received signal \mathbf{y} without taking care of the combination coefficient of \mathbf{x}_1 and \mathbf{x}_2 . Hence, we do not need to use the C&F protocol.

Next, we compare the achievable rate obtained from Theorem 1 with the achievable rate derived in [1], denoted as,

$$R_{PIR}^{C\&F} = \frac{1}{2} \log^+ \left(\frac{1 + P(\tilde{h}_1^2 + \tilde{h}_2^2)}{\|\mathbf{a}\|^2 + P(a_1 \tilde{h}_2 - a_2 \tilde{h}_1)^2} \right) \quad (15)$$

Both rates show favorable scaling behavior as the number of servers N increases. However, it is evident (see Figure 2) that $R_{PIR}^{C\&F}$ does not scale efficiently with the power P . At the same time, R_{PIR}^{eq} demonstrates superior scaling characteristics with respect to P (More details and empirical results are provided in Appendix C). The inefficiency in the scaling of $R_{PIR}^{C\&F}$ with P arises from a term in its denominator that depends on P .

Another thing to be aware of is the computational complexity of the scheme. To achieve the maximum rate in (15), one should note that the user may choose \mathcal{S}_1 , \mathcal{S}_2 , and the coefficient vector \mathbf{a} to maximize it. Namely, we have the following global optimization problem,

$$\max_{\substack{\mathcal{S}_1, \mathcal{S}_2, \mathbf{a} \\ a_j \neq 0}} \left\{ \frac{1}{2} \log^+ \left(\frac{1 + P \left(\left(\sum_{k \in \mathcal{S}_1} h_k \right)^2 + \left(\sum_{k \in \mathcal{S}_2} h_k \right)^2 \right)}{\|\mathbf{a}\|^2 + P \left(a_1 \sum_{k \in \mathcal{S}_2} h_k - a_2 \sum_{k \in \mathcal{S}_1} h_k \right)^2} \right) \right\}. \quad (16)$$

In the above optimization, finding the optimal partition and coefficient vector \mathbf{a} is a hard problem. Even for a fixed \mathbf{a} , the problem relates to the subset sum problem (or partition problem), which is NP-complete [24]. However, to maximize the rate in Theorem 1, the user only needs to find the best partition.

VI. CONCLUSION

This study presents a PIR scheme explicitly designed for the block fading AWGN MAC. Our proposed scheme surpasses this model's previously established best-known achievable rate for PIR. Notably, our approach maintains a finite gap from the channel capacity as N grows sufficiently large. Moreover, it exhibits favorable scalability concerning the number of databases and the power P .

While our contributions significantly advance the understanding of PIR in the block-fading AWGN MAC, determining the PIR capacity for this specific problem remains an intriguing open challenge. Future work could explore designing PIR schemes for block-fading AWGN MAC with CSI available only at the receiver.

APPENDIX A PROOF OF LEMMA 1

Proof. The proof is by using a sub-optimal, random construction for the two sets. We construct \mathcal{S}_1 and \mathcal{S}_2 to be sets of size $\lfloor N/2 \rfloor$, chosen uniformly from \mathbf{h} without repetition, i.e., $\mathcal{S}_1 \cap \mathcal{S}_2 = \emptyset$. Assume, without loss of generality, $\tilde{h}_1 \leq \tilde{h}_2$. Note that if N is even, we have $\sum_{k=1}^N |h_k| = \tilde{h}_1 + \tilde{h}_2$. If N

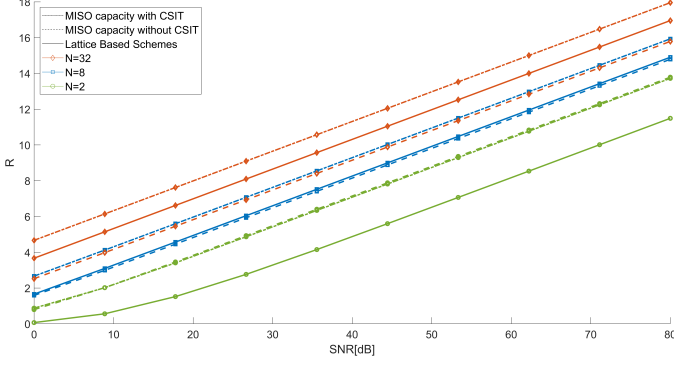


Fig. 3: The average PIR rate as a function of the SNR

is odd, we have $\sum_{k=1}^N |h_k| = \tilde{h}_1 + \tilde{h}_2 + |h_l|$ for some random index $1 \leq l \leq N$, which is not contained in \mathcal{S}_1 and \mathcal{S}_2 . Then,

$$\begin{aligned}
C_{SR}^{MISO} &= \max_{\substack{\mathcal{S}_1, \mathcal{S}_2 \\ \tilde{h}_1 \leq \tilde{h}_2}} \left\{ \frac{1}{2} \log^+ \left(\frac{1}{2} + \left(\sum_{k \in \mathcal{S}_1} h_k \right)^2 P \right) \right\} \\
&\leq \frac{1}{2} \log \left(1 + P \left(\sum_{k=1}^N |h_k| \right)^2 \right) - \frac{1}{2} \log^+ \left(\frac{1}{2} + \tilde{h}_1^2 P \right) \\
&\stackrel{(a)}{\leq} \frac{1}{2} \log \left(\frac{1 + P \left(\tilde{h}_1 + \tilde{h}_2 + |h_l| \right)^2}{\frac{1}{2} + \tilde{h}_1^2 P} \right) \\
&= \frac{1}{2} + \frac{1}{2} \log \left(\frac{1 + P \left(2\tilde{h}_2 + |h_l| \right)^2}{1 + 2\tilde{h}_1^2 P} \right) \\
&\leq \frac{1}{2} + \frac{1}{2} \log \left(2 \frac{\tilde{h}_2^2}{\tilde{h}_1^2} + \frac{1 + 4\tilde{h}_2|h_l|P + h_l^2 P}{1 + 2\tilde{h}_1^2 P} \right),
\end{aligned}$$

where (a) follows since $\log^+(x) \geq \log(x)$. Note that the elements in \mathcal{S}_1 and \mathcal{S}_2 are i.i.d. random variables with a Half-Normal distribution, mean $\sqrt{\frac{2}{\pi}}$ and variance $1 - \frac{2}{\pi}$. Each set contains $\lfloor N/2 \rfloor$ elements. Hence, By the strong law of large numbers (SLLN), we have $\frac{\tilde{h}_i}{\lfloor N/2 \rfloor} \xrightarrow{N \rightarrow \infty} \sqrt{\frac{2}{\pi}}$ for $i = 1, 2$. Note also that

$$\frac{1 + 4\tilde{h}_2 h_l P + h_l^2 P}{1 + 2\tilde{h}_1^2 P} \xrightarrow{N \rightarrow \infty} 0.$$

Since $\log(2+x) = \log(2) + \frac{x}{2} + O(x^2)$, we have

$$C_{SR}^{MISO} - \max_{\substack{\mathcal{S}_1, \mathcal{S}_2 \\ \tilde{h}_1 \leq \tilde{h}_2}} \{R_{PIR}^{eq}\} \leq 1 + O\left(\frac{1}{N}\right).$$

□

APPENDIX B

LOWER BOUND ON THE EXPECTED ACHIEVABLE RATE

Proof: Pick \mathcal{S}_1 and \mathcal{S}_2 as follow. We construct \mathcal{S}_1 to be a set of size $\frac{N}{2}$, chosen uniformly from all the elements of $|\mathbf{h}|$, and \mathcal{S}_2 to be a set of size $\frac{N}{2}$ of all the others elements

from $|\mathbf{h}|$. The reason we use the absolute value of \mathbf{h} is that we want to sum up the coefficient for gain. We assume CSI at the receiver. Hence, we can control the sign of the transmitting signal at each server by sending a sign bit to each (depending on the channel coefficient sign). Given \mathcal{S}_1 and \mathcal{S}_2 , compute the vector $\tilde{\mathbf{h}} = (\tilde{h}_1, \tilde{h}_2)$. we start with (13),

$$\begin{aligned}
&\mathbb{E} \left[R_{PIR}^{J,max} \right] \\
&= \mathbb{E} \left[\max_{\substack{\mathcal{S}_1, \mathcal{S}_2 \\ \tilde{h}_1 \leq \tilde{h}_2}} \left\{ \frac{1}{2} \log^+ \left(\frac{1}{2} + \tilde{h}_1^2 P \right) \right\} \right] \\
&\stackrel{(a)}{\geq} \mathbb{E} \left[\frac{1}{2} \log \left(\frac{1}{2} + \tilde{h}_1^2 P \right) \right] \\
&\stackrel{(b)}{\geq} \mathbb{E} \left[\frac{1}{2} \log \left(1 + 2\tilde{h}_1^2 P \right) \right] - \frac{1}{2} \\
&\stackrel{(c)}{\geq} \mathbb{E} \left[\frac{1}{2} \log \left(1 + 2\tilde{h}_1^2 P \right) \middle| \left| \frac{2}{N} \tilde{h}_1^* - \sqrt{\frac{2}{\pi}} \right| \leq \epsilon \right] \\
&\quad \cdot Pr \left(\left| \frac{2}{N} \tilde{h}_1^* - \sqrt{\frac{2}{\pi}} \right| \leq \epsilon \right) \\
&\quad + \mathbb{E} \left[\frac{1}{2} \log \left(1 + 2\tilde{h}_1^2 P \right) \middle| \left| \frac{2}{N} \tilde{h}_1^* - \sqrt{\frac{2}{\pi}} \right| > \epsilon \right] \\
&\quad \cdot Pr \left(\left| \frac{2}{N} \tilde{h}_1^* - \sqrt{\frac{2}{\pi}} \right| > \epsilon \right) - \frac{1}{2} \\
&\geq \mathbb{E} \left[\frac{1}{2} \log \left(1 + 2\tilde{h}_1^2 P \right) \middle| \left| \frac{2}{N} \tilde{h}_1^* - \sqrt{\frac{2}{\pi}} \right| \leq \epsilon \right] \\
&\quad \cdot Pr \left(\left| \frac{2}{N} \tilde{h}_1^* - \sqrt{\frac{2}{\pi}} \right| \leq \epsilon \right) - \frac{1}{2} \\
&\stackrel{(d)}{\geq} \frac{1}{2} \log \left(1 + 2 \frac{N^2 P}{4} \left(\sqrt{\frac{2}{\pi}} - \epsilon \right)^2 \right) \\
&\quad \cdot Pr \left(\left| \frac{2}{N} \tilde{h}_1^* - \sqrt{\frac{2}{\pi}} \right| \leq \epsilon \right) - \frac{1}{2} \\
&\stackrel{(e)}{\geq} \frac{1}{2} \log \left(1 + 2 \frac{N^2 P}{4} \left(\sqrt{\frac{2}{\pi}} - \epsilon \right)^2 \right) \\
&\quad \cdot \left(1 - \frac{Var \left(\frac{2}{N} \tilde{h}_1^* \right)}{\epsilon^2} \right) - \frac{1}{2} \\
&\stackrel{(f)}{\geq} \frac{1}{2} \log \left(1 + 2 \frac{N^2 P}{4} \left(\sqrt{\frac{2}{\pi}} - \epsilon \right)^2 \right) \\
&\quad \cdot \left(1 - \frac{2(1 - \frac{2}{\pi})}{N\epsilon^2} \right) - \frac{1}{2} \\
&= \frac{1}{2} \log \left(\frac{2(2 + N^2 P \epsilon)}{4} \right) - \frac{1}{2} - o(1)
\end{aligned}$$

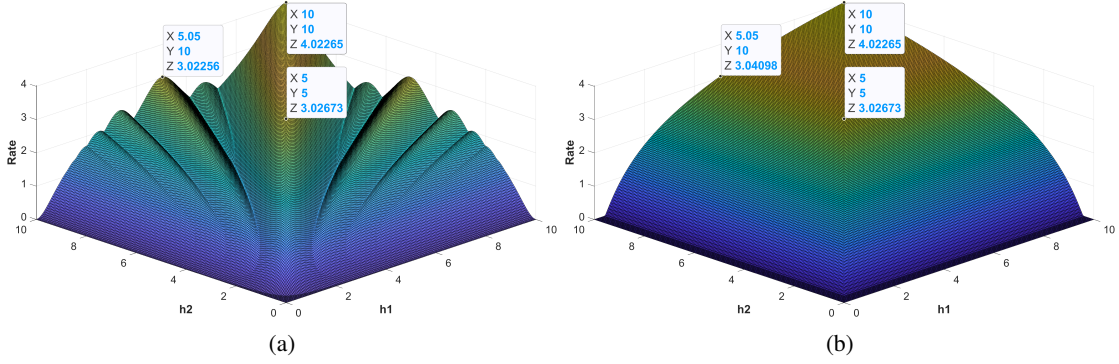


Fig. 4: The graphs shows the rates for different \tilde{h}_1 and \tilde{h}_2 . graph (a) is for $R_{PIR}^{C\&F}$ and graph (b) for R_{PIR}^{eq} where $P=5$.

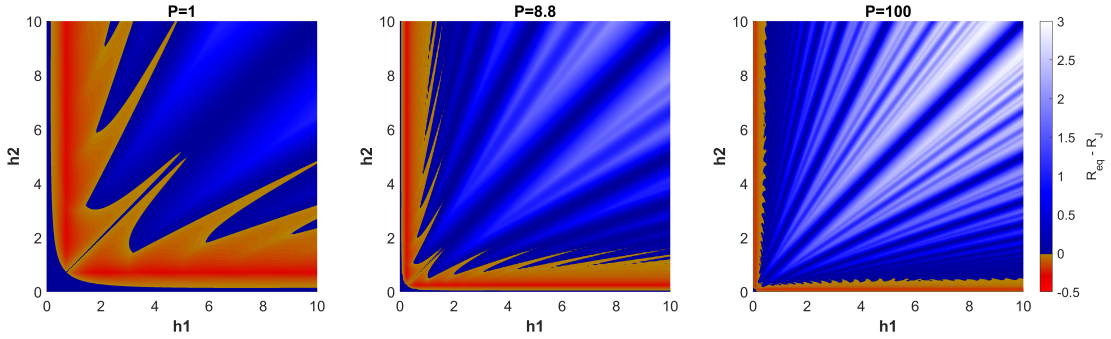


Fig. 5: The graphs shows the difference between R_{PIR}^{eq} to $R_{PIR}^{C\&F}$ for different \tilde{h}_1 and \tilde{h}_2 . Blue colors for positive values and red colors for negative values. Each graph is evaluated for different Powers.

$$= \frac{1}{2} \log \left(\frac{2 + N^2 P c}{4} \right) - o(1)$$

(a) follows from the suboptimal choice for \mathcal{S}_1 and \mathcal{S}_2 where we denote this choice by $(\cdot)^*$. In addition, note that $\log^+(x) \geq \log(x)$. (b) follow by throwing away a positive element. (c) due to the law of total probability. (d) follows since $\left| \frac{2}{N} \tilde{h}_1^* - \sqrt{\frac{2}{\pi}} \right| \leq \epsilon$ and thus $\tilde{h}_1^* \geq \frac{N}{2} \left(\sqrt{\frac{2}{\pi}} - \epsilon \right)$. we also need to set $\sqrt{\frac{2}{\pi}} - \epsilon \geq 0$ in order to get $\tilde{h}_1^{*2} \geq \left(\frac{N}{2} \left(\sqrt{\frac{2}{\pi}} - \epsilon \right) \right)^2$. (e) and (f) follows from $Var(\tilde{h}_1^*) = Var(\sum_{k \in \mathcal{S}_1} h_k) = \frac{N'}{2} \left(1 - \frac{2}{\pi} \right)$ since the elements in \mathcal{S}_1 are *i.i.d.* random variables distributed as Half-Normal distribution with mean $\sqrt{\frac{2}{\pi}}$ and variance $1 - \frac{2}{\pi}$. In addition to Chebyshev's inequality where we require that $\sqrt{\frac{2}{N} \left(1 - \frac{2}{\pi} \right)} < \epsilon < \sqrt{\frac{2}{\pi}}$. Any ϵ outside this interval will lead to a meaningless result. Thus, we set it to $\epsilon = 0.5$ and we denote $c = \left(\sqrt{\frac{2}{\pi}} - \frac{1}{2} \right)^2$. ■

APPENDIX C

EMPIRICAL SIMULATION RESULTS

Fig. 4 depicts the achievable rates under various channel coefficients to visualize the rate behavior. In contrast to R_{PIR}^{eq} , it can be observed that $R_{PIR}^{C\&F}$ is not monotonically increasing as it approaches the line $\tilde{h}_1 = \tilde{h}_2$ and actually achieves a lower rate in most of the plane.

Furthermore, empirical simulation results indicate that as P tends to infinity, $R_{PIR}^{C\&F} \leq R_{PIR}^{eq}$. Fig.5 depicts the difference

of $R_{PIR}^{eq} - R_{PIR}^{C\&F}$ as a function of \tilde{h}_1 and \tilde{h}_2 . The blue region represents a positive difference, while the red region represents a negative difference. The graph shows that R_{PIR}^{eq} overcomes $R_{PIR}^{C\&F}$ as the power P increases.

REFERENCES

- [1] O. Shmuel and A. Cohen, "Private information retrieval over gaussian MAC," *IEEE Transactions on Information Theory*, vol. 67, no. 8, pp. 5404–5419, 2021.
- [2] W. Gasarch, "A survey on private information retrieval," *Bulletin of the EATCS*, vol. 82, no. 72–107, p. 113, 2004.
- [3] R. Ostrovsky and W. E. Skeith, "A survey of single-database private information retrieval: Techniques and applications," in *International Workshop on Public Key Cryptography*. Springer, 2007, pp. 393–411.
- [4] S. Yekhanin, "Private information retrieval," in *Locally Decodable Codes and Private Information Retrieval Schemes*. Springer, 2010, pp. 61–74.
- [5] Z. Wang and S. Ulukus, "Fully robust federated submodel learning in a distributed storage system," *arXiv preprint arXiv:2306.05402*, 2023.
- [6] S. Vithana and S. Ulukus, "Efficient private federated submodel learning," in *ICC 2022-IEEE International Conference on Communications*. IEEE, 2022, pp. 3394–3399.
- [7] M. Kim and J. Lee, "Information-theoretic privacy in federated submodel learning," *ICT express*, 2022.
- [8] B. Chor, O. Goldreich, E. Kushilevitz, and M. Sudan, "Private information retrieval," in *Proceedings of IEEE 36th Annual Foundations of Computer Science*. IEEE, 1995, pp. 41–50.
- [9] H. Sun and S. A. Jafar, "The capacity of private information retrieval," *IEEE Transactions on Information Theory*, vol. 63, no. 7, pp. 4075–4088, 2017.
- [10] —, "The capacity of robust private information retrieval with colluding databases," *IEEE Transactions on Information Theory*, vol. 64, no. 4, pp. 2361–2370, 2017.

- [11] R. Tajeddine, O. W. Gnilke, D. Karpuk, R. Freij-Hollanti, C. Hollanti, and S. El Rouayheb, "Private information retrieval schemes for coded data with arbitrary collusion patterns," in *2017 IEEE International Symposium on Information Theory (ISIT)*. IEEE, 2017, pp. 1908–1912.
- [12] K. Banawan and S. Ulukus, "The capacity of private information retrieval from byzantine and colluding databases," *IEEE Transactions on Information Theory*, vol. 65, no. 2, pp. 1206–1219, 2018.
- [13] H. Sun and S. A. Jafar, "The capacity of symmetric private information retrieval," *IEEE Transactions on Information Theory*, vol. 65, no. 1, pp. 322–329, 2018.
- [14] T. H. Chan, S.-W. Ho, and H. Yamamoto, "Private information retrieval for coded storage," in *2015 IEEE International Symposium on Information Theory (ISIT)*. IEEE, 2015, pp. 2842–2846.
- [15] R. Tajeddine, O. W. Gnilke, and S. El Rouayheb, "Private information retrieval from MDS coded data in distributed storage systems," *IEEE Transactions on Information Theory*, vol. 64, no. 11, pp. 7081–7093, 2018.
- [16] K. Banawan and S. Ulukus, "The capacity of private information retrieval from coded databases," *IEEE Transactions on Information Theory*, vol. 64, no. 3, pp. 1945–1956, 2018.
- [17] J. Zhu, Q. Yan, C. Qi, and X. Tang, "A new capacity-achieving private information retrieval scheme with (almost) optimal file length for coded servers," *IEEE Transactions on Information Forensics and Security*, vol. 15, pp. 1248–1260, 2019.
- [18] R. Zhou, C. Tian, H. Sun, and T. Liu, "Capacity-achieving private information retrieval codes from mds-coded databases with minimum message size," *IEEE Transactions on Information Theory*, vol. 66, no. 8, pp. 4904–4916, 2020.
- [19] K. Banawan and S. Ulukus, "Noisy private information retrieval: On separability of channel coding and information retrieval," *IEEE Transactions on Information Theory*, vol. 65, no. 12, pp. 8232–8249, 2019.
- [20] B. Nazer and M. Gastpar, "Compute-and-Forward: Harnessing interference through structured codes," *IEEE Transactions on Information Theory*, vol. 57, no. 10, pp. 6463–6486, 2011.
- [21] U. Erez and R. Zamir, "Achieving $1/2 \log(1 + \text{SNR})$ on the AWGN channel with lattice encoding and decoding," *IEEE Transactions on Information Theory*, vol. 50, no. 10, pp. 2293–2314, 2004.
- [22] T. M. Cover and J. A. Thomas, *Elements of information theory*. John Wiley & Sons, 2012.
- [23] M. Vu, "MISO capacity with per-antenna power constraint," *IEEE Transactions on Communications*, vol. 59, no. 5, pp. 1268–1274, 2011.
- [24] T. H. Cormen, C. E. Leiserson, R. L. Rivest, and C. Stein, *Introduction to algorithms*. MIT press, 2009.

An Efficient, High-Rate Scheme for Private Information Retrieval over the Gaussian MAC

Or Elimelech and Asaf Cohen
Department of Electrical & Computer Engineering
Ben-Gurion University of the Negev Beersheba, Israel

APPENDIX A PROOF OF LEMMA ??

Proof. The proof is by using a sub-optimal, random construction for the two sets. We construct \mathcal{S}_1 and \mathcal{S}_2 to be sets of size $\lfloor N/2 \rfloor$, chosen uniformly from \mathbf{h} without repetition, i.e., $\mathcal{S}_1 \cap \mathcal{S}_2 = \emptyset$. Assume, without loss of generality, $\tilde{h}_1 \leq \tilde{h}_2$. Note that if N is even, we have $\sum_{k=1}^N |h_k| = \tilde{h}_1 + \tilde{h}_2$. If N is odd, we have $\sum_{k=1}^N |h_k| = \tilde{h}_1 + \tilde{h}_2 + |h_l|$ for some random index $1 \leq l \leq N$, which is not contained in \mathcal{S}_1 and \mathcal{S}_2 . Then,

$$\begin{aligned} C_{SR}^{MISO} - \max_{\substack{\mathcal{S}_1, \mathcal{S}_2 \\ \tilde{h}_1 \leq \tilde{h}_2}} & \left\{ \frac{1}{2} \log^+ \left(\frac{1}{2} + \left(\sum_{k \in \mathcal{S}_1} h_k \right)^2 P \right) \right\} \\ & \leq \frac{1}{2} \log \left(1 + P \left(\sum_{k=1}^N |h_k| \right)^2 \right) - \frac{1}{2} \log^+ \left(\frac{1}{2} + \tilde{h}_1^2 P \right) \\ & \stackrel{(a)}{\leq} \frac{1}{2} \log \left(\frac{1 + P \left(\tilde{h}_1 + \tilde{h}_2 + |h_l| \right)^2}{\frac{1}{2} + \tilde{h}_1^2 P} \right) \\ & = \frac{1}{2} + \frac{1}{2} \log \left(\frac{1 + P \left(2\tilde{h}_2 + |h_l| \right)^2}{1 + 2\tilde{h}_1^2 P} \right) \\ & \leq \frac{1}{2} + \frac{1}{2} \log \left(2 \frac{\tilde{h}_2^2}{\tilde{h}_1^2} + \frac{1 + 4\tilde{h}_2|h_l|P + h_l^2 P}{1 + 2\tilde{h}_1^2 P} \right), \end{aligned}$$

where (a) follows since $\log^+(x) \geq \log(x)$. Note that the elements in \mathcal{S}_1 and \mathcal{S}_2 are i.i.d. random variables with a Half-Normal distribution, mean $\sqrt{\frac{2}{\pi}}$ and variance $1 - \frac{2}{\pi}$. Each set contains $\lfloor N/2 \rfloor$ elements. Hence, By the strong law of large numbers (SLLN), we have $\frac{\tilde{h}_i}{\lfloor N/2 \rfloor} \xrightarrow{N \rightarrow \infty} \sqrt{\frac{2}{\pi}}$ for $i = 1, 2$. Note also that

$$\frac{1 + 4\tilde{h}_2 h_l P + h_l^2 P}{1 + 2\tilde{h}_1^2 P} \xrightarrow{N \rightarrow \infty} 0.$$

Since $\log(2 + x) = \log(2) + \frac{x}{2} + O(x^2)$, we have

$$C_{SR}^{MISO} - \max_{\substack{\mathcal{S}_1, \mathcal{S}_2 \\ \tilde{h}_1 \leq \tilde{h}_2}} \{R_{PIR}^{eq}\} \leq 1 + O\left(\frac{1}{N}\right).$$

□

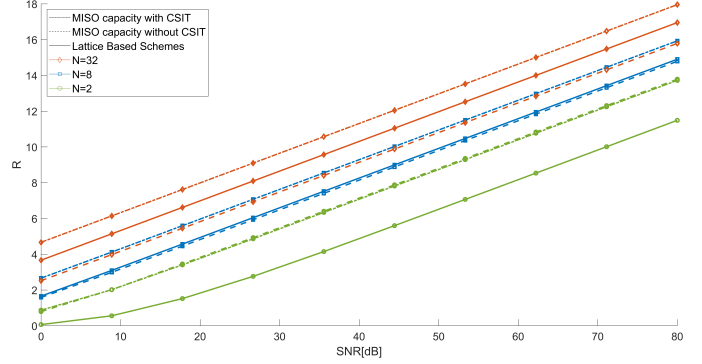


Fig. 1: The average PIR rate as a function of the SNR

APPENDIX B LOWER BOUND ON THE EXPECTED ACHIEVABLE RATE

Proof: Pick \mathcal{S}_1 and \mathcal{S}_2 as follow. We construct \mathcal{S}_1 to be a set of size $\frac{N}{2}$, chosen uniformly from all the elements of $|\mathbf{h}|$, and \mathcal{S}_2 to be a set of size $\frac{N}{2}$ of all the others elements from $|\mathbf{h}|$. The reason we use the absolute value of \mathbf{h} is that we want to sum up the coefficient for gain. We assume CSI at the receiver. Hence, we can control the sign of the transmitting signal at each server by sending a sign bit to each (depending on the channel coefficient sign). Given \mathcal{S}_1 and \mathcal{S}_2 , compute the vector $\tilde{\mathbf{h}} = (\tilde{h}_1, \tilde{h}_2)$. we start with (??),

$$\begin{aligned} & \mathbb{E} \left[R_{PIR}^{J,max} \right] \\ & = \mathbb{E} \left[\max_{\substack{\mathcal{S}_1, \mathcal{S}_2 \\ \tilde{h}_1 \leq \tilde{h}_2}} \left\{ \frac{1}{2} \log^+ \left(\frac{1}{2} + \tilde{h}_1^2 P \right) \right\} \right] \\ & \stackrel{(a)}{\geq} \mathbb{E} \left[\frac{1}{2} \log \left(\frac{1}{2} + \tilde{h}_1^2 P \right) \right] \\ & \stackrel{(b)}{\geq} \mathbb{E} \left[\frac{1}{2} \log \left(1 + 2\tilde{h}_1^2 P \right) \right] - \frac{1}{2} \\ & \stackrel{(c)}{\geq} \mathbb{E} \left[\frac{1}{2} \log \left(1 + 2\tilde{h}_1^2 P \right) \middle| \left| \frac{2}{N} \tilde{h}_1^* - \sqrt{\frac{2}{\pi}} \right| \leq \epsilon \right] \\ & \quad \cdot \Pr \left(\left| \frac{2}{N} \tilde{h}_1^* - \sqrt{\frac{2}{\pi}} \right| \leq \epsilon \right) \\ & \quad + \mathbb{E} \left[\frac{1}{2} \log \left(1 + 2\tilde{h}_1^2 P \right) \middle| \left| \frac{2}{N} \tilde{h}_1^* - \sqrt{\frac{2}{\pi}} \right| > \epsilon \right] \end{aligned}$$

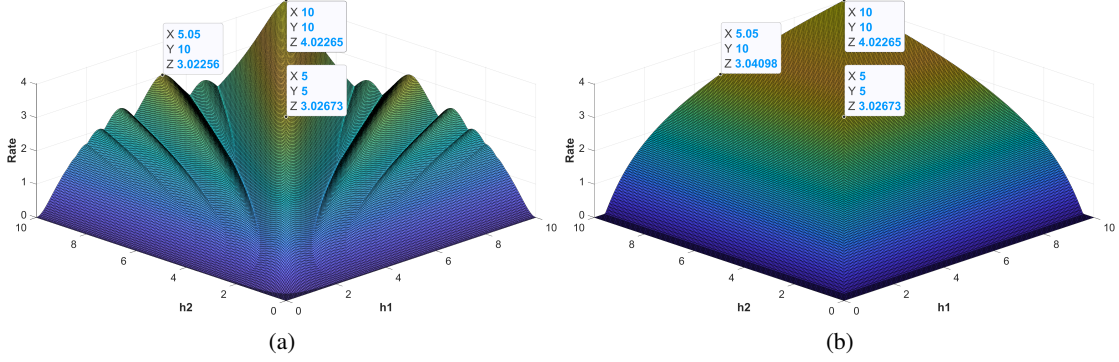


Fig. 2: The graphs shows the rates for different \tilde{h}_1 and \tilde{h}_2 . graph (a) is for $R_{PIR}^{C\&F}$ and graph (b) for R_{PIR}^{eq} where $P=5$.

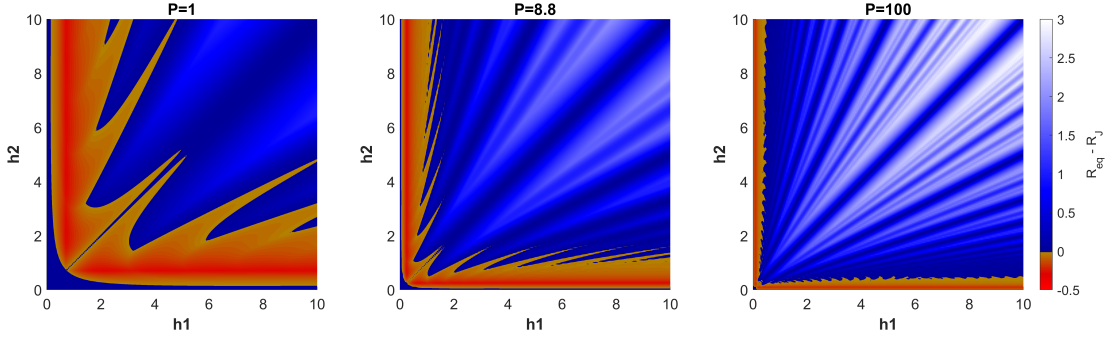


Fig. 3: The graphs shows the difference between R_{PIR}^{eq} to $R_{PIR}^{C\&F}$ for different \tilde{h}_1 and \tilde{h}_2 . Blue colors for positive values and red colors for negative values. Each graph is evaluated for different Powers.

$$\begin{aligned}
& \cdot \Pr \left(\left| \frac{2}{N} \tilde{h}_1^* - \sqrt{\frac{2}{\pi}} \right| > \epsilon \right) - \frac{1}{2} \\
& \geq \mathbb{E} \left[\frac{1}{2} \log \left(1 + 2 \tilde{h}_1^{*2} P \right) \middle| \left| \frac{2}{N} \tilde{h}_1^* - \sqrt{\frac{2}{\pi}} \right| \leq \epsilon \right] \\
& \quad \cdot \Pr \left(\left| \frac{2}{N} \tilde{h}_1^* - \sqrt{\frac{2}{\pi}} \right| \leq \epsilon \right) - \frac{1}{2} \\
& \stackrel{(d)}{\geq} \frac{1}{2} \log \left(1 + 2 \frac{N^2 P}{4} \left(\sqrt{\frac{2}{\pi}} - \epsilon \right)^2 \right) \\
& \quad \cdot \Pr \left(\left| \frac{2}{N} \tilde{h}_1^* - \sqrt{\frac{2}{\pi}} \right| \leq \epsilon \right) - \frac{1}{2} \\
& \stackrel{(e)}{\geq} \frac{1}{2} \log \left(1 + 2 \frac{N^2 P}{4} \left(\sqrt{\frac{2}{\pi}} - \epsilon \right)^2 \right) \\
& \quad \cdot \left(1 - \frac{\text{Var} \left(\frac{2}{N} \tilde{h}_1^* \right)}{\epsilon^2} \right) - \frac{1}{2} \\
& \stackrel{(f)}{\geq} \frac{1}{2} \log \left(1 + 2 \frac{N^2 P}{4} \left(\sqrt{\frac{2}{\pi}} - \epsilon \right)^2 \right) \\
& \quad \cdot \left(1 - \frac{2(1 - \frac{2}{\pi})}{N \epsilon^2} \right) - \frac{1}{2}
\end{aligned}$$

$$\begin{aligned}
& = \frac{1}{2} \log \left(\frac{2(2 + N^2 P c)}{4} \right) - \frac{1}{2} - o(1) \\
& = \frac{1}{2} \log \left(\frac{2 + N^2 P c}{4} \right) - o(1)
\end{aligned}$$

(a) follows from the suboptimal choice for S_1 and S_2 where we denote this choice by $(\cdot)^*$. In addition, note that $\log^+(x) \geq \log(x)$. (b) follow by throwing away a positive element. (c) due to the law of total probability. (d) follows since $\left| \frac{2}{N} \tilde{h}_1^* - \sqrt{\frac{2}{\pi}} \right| \leq \epsilon$ and thus $\tilde{h}_1^* \geq \frac{N}{2} \left(\sqrt{\frac{2}{\pi}} - \epsilon \right)$. we also need to set $\sqrt{\frac{2}{\pi}} - \epsilon \geq 0$ in order to get $\tilde{h}_1^{*2} \geq \left(\frac{N}{2} \left(\sqrt{\frac{2}{\pi}} - \epsilon \right) \right)^2$. (e) and (f) follows from $\text{Var}(\tilde{h}_1^*) = \text{Var}(\sum_{k \in S_1} h_k) = \frac{N'}{2} \left(1 - \frac{2}{\pi} \right)$ since the elements in S_1 are *i.i.d.* random variables distributed as Half-Normal distribution with mean $\sqrt{\frac{2}{\pi}}$ and variance $1 - \frac{2}{\pi}$. In addition to Chebyshev's inequality where we require that $\sqrt{\frac{2}{N} \left(1 - \frac{2}{\pi} \right)} < \epsilon < \sqrt{\frac{2}{\pi}}$. Any ϵ outside this interval will lead to a meaningless result. Thus, we set it to $\epsilon = 0.5$ and we denote $c = \left(\sqrt{\frac{2}{\pi}} - \frac{1}{2} \right)^2$. ■

APPENDIX C EMPIRICAL SIMULATION RESULTS

Fig. 2 depicts the achievable rates under various channel coefficients to visualize the rate behavior. In contrast to R_{PIR}^{eq} , it can be observed that $R_{PIR}^{C\&F}$ is not monotonically increasing

as it approaches the line $\tilde{h}_1 = \tilde{h}_2$ and actually achieves a lower rate in most of the plane.

Furthermore, empirical simulation results indicate that as P tends to infinity, $R_{PIR}^{C\&F} \leq R_{PIR}^{eq}$. Fig.3 depicts the difference of $R_{PIR}^{eq} - R_{PIR}^{C\&F}$ as a function of \tilde{h}_1 and \tilde{h}_2 . The blue region represents a positive difference, while the red region represents a negative difference. The graph shows that R_{PIR}^{eq} overcomes $R_{PIR}^{C\&F}$ as the power P increases.